

Formula for proton-nucleus reaction cross section at intermediate energies and its application

Kei Iida,¹ Akihisa Kohama,² and Kazuhiro Oyamatsu^{2,3}

¹*RIKEN BNL Research Center, Physics Department,
Brookhaven National Laboratory, Upton, New York 11973-5000, USA*

¹*RIKEN (The Institute of Physical and Chemical Research),
2-1 Hirosawa, Wako-shi, Saitama 351-0198, Japan*

³*Department of Media Theories and Production, Aichi Shukutoku University,
Nagakute, Nagakute-cho, Aichi-gun, Aichi 480-1197, Japan*

(Dated: December 2, 2024)

We construct a formula for proton-nucleus total reaction cross section as a function of the mass and neutron excess of the target nucleus and the proton incident energy. We deduce the dependence of the cross section on the mass number and the proton incident energy from a simple argument involving the proton optical depth within the framework of a black sphere approximation of nuclei, while we describe the neutron excess dependence by introducing the density derivative of the symmetry energy, L , on the basis of a radius formula constructed from macroscopic nuclear models. We find that the cross section formula can reproduce the energy dependence of the cross section measured for stable nuclei without introducing any adjustable energy dependent parameter. We finally discuss whether or not the reaction cross section is affected by an extremely low density tail of the neutron distribution for halo nuclei.

PACS numbers: 25.40.Ep, 21.10.Gv, 24.10.Ht, 25.60.Dz

I. INTRODUCTION

The nuclear size and mass are fundamental quantities characterizing the bulk properties of nuclei. In fact, the saturation of the binding energy and density deduced from systematic data for masses and charge radii of stable nuclei reflects the behavior of the equation of state of nearly symmetric nuclear matter near the saturation density n_0 . Extension of such data to a more neutron-rich regime opens up an opportunity of probing the equation of state of asymmetric nuclear matter. One of the poorly known parameters characterizing such an equation of state is the density symmetry coefficient, $L \equiv 3n_0 dS/dn|_{n_0}$, with the nucleon density n and the density dependent symmetry energy $S(n)$. The sensitivity of L to the structure and evolution of neutron stars and to nuclear structure and reactions has been discussed in Ref. [1]. This parameter is expected to be deduced from future systematic data for unstable nuclei because macroscopic nuclear models yield a clear correlation between the root-mean-square (rms) matter radii of very neutron-rich nuclei and L mainly through the L dependence of the saturation density of asymmetric nuclear matter [2].

For stable nuclei, electron and proton elastic scattering data have been obtained systematically, from which the charge and matter density distributions can be fairly well deduced [3, 4, 5, 6, 7], while for unstable nuclei, not only do electron elastic scattering experiments have yet to be performed, but also proton scattering data obtained from radioactive ion beams incident on a proton target [8, 9] are very limited. Instead of relying on such elastic scattering data, deduction of the rms matter radius of unstable nuclei has been often performed

through measurements of reaction/interaction cross section (e.g., Ref. [10]). However, the relation between the reaction/interaction cross section and the matter radius is not obvious theoretically and in fact is quite model dependent.

Recently we systematically analyzed the proton elastic scattering and reaction cross section data for stable nuclei at proton incident energy of ~ 800 – 1000 MeV on the basis of a black sphere picture of nuclei [11, 12]. This picture is originally expected to give a decent description of the reaction cross section for any kind of incident particle that tends to be attenuated in the nuclear interiors. In fact we showed that for proton beams incident on stable nuclei, the cross section of the black sphere of radius a , which was determined by fitting the angle of the first elastic diffraction peak calculated for the proton diffraction by a circular black disk of radius a to the measured value, is consistent with the measured reaction cross section [12]. We also showed that for stable nuclei of mass number $A > 50$, the quantity $\sqrt{3/5}a$ agrees with the rms matter radius deduced in previous elaborate analyses from the proton elastic scattering data within error bars [11]. These salient features of the black sphere picture could help deduce the density dependence of the symmetry energy from future systematic data on the reaction cross section and proton elastic scattering for unstable nuclei.

In this work we construct a formula for the proton-nucleus total reaction cross section as a function of the target mass number A , the proton incident energy T_p , and the target neutron excess $\delta = 1 - 2Z/A$. The dependence of the cross section on A and T_p , which is deduced by combining the black sphere picture of nuclei with a simple argument involving the proton optical depth, is remarkably consistent with the empirical data for stable nuclei at $T_p = 100$ – 1000 MeV. Bearing in mind future

possible data for unstable nuclei at intermediate energies, we then describe the neutron excess dependence by using a radius formula [2] constructed from macroscopic nuclear models in terms of L . As a possible application of the formula, we discuss the effect of nuclear deformation and neutron halos on the reaction cross section. We finally extend the formula to the case of nucleus-nucleus reaction cross section and compare the result with the existing data.

II. FORMULA FOR PROTON-NUCLEUS REACTION CROSS SECTION

We start with a formula for the reaction cross section for protons on stable nuclei as a function of A and T_p . For this purpose we note the black sphere picture [11] in which the black sphere radius a is determined from $2pa \sin(\theta_M/2) = 5.1356 \dots$ with the proton incident momentum in the center-of-mass frame, p , and the first peak angle for the measured diffraction in proton-nucleus elastic scattering, θ_M . We then recall the known properties from the black sphere picture for $T_p = 800\text{--}1000$ MeV [12]: (i) the black sphere radius a globally behaves as $1.214A^{1/3}$ fm. (ii) the measured σ_R agrees with πa^2 within error bars. We also note that $\sigma_R \approx \pi a^2$ is satisfied for the values of T_p down to about 100 MeV [13] and that σ_R is nearly flat at least for $T_p = 100\text{--}1000$ MeV [14]. It is thus natural to set

$$\sigma_R = \pi a_0^2 \left(1 + \frac{\Delta a}{a_0}\right)^2, \quad (1)$$

where a_0 is the black sphere radius at $T_p = 800$ MeV, and Δa is the deviation of a from a_0 at given T_p above 100 MeV. In this setting, we assume that the incident protons are point particles, leading to vanishing cross section for the proton-proton case. This is reasonable since the measured proton-proton reaction cross section is relatively small at $T_p \lesssim 1000$ MeV [15, 16].

In deriving the expression for Δa , we focus on the “optical” depth for incident protons. Note that in a real situation, the black sphere radius a corresponds to a critical radius inside which the protons are attenuated in a target nucleus. More explicitly, the optical depth for the protons,

$$\int_l dl [\sigma_{pn} n_n(\mathbf{r}) + \sigma_{pp} n_p(\mathbf{r})], \quad (2)$$

amounts to a critical value when the nearest distance between the proton trajectory and the nuclear target is a . Here l is the proton trajectory, $n_N(\mathbf{r})$ is the point N -nucleon density, and σ_{pN} is the empirical pN total cross section (e.g., Refs. [15, 16, 17]). Let us now approximate the trajectory, although it is slightly distorted by the Coulomb repulsion, by a straight line. We also approximate the nucleon distributions by a trapezoidal form of the length of the bottom, R , and that of the

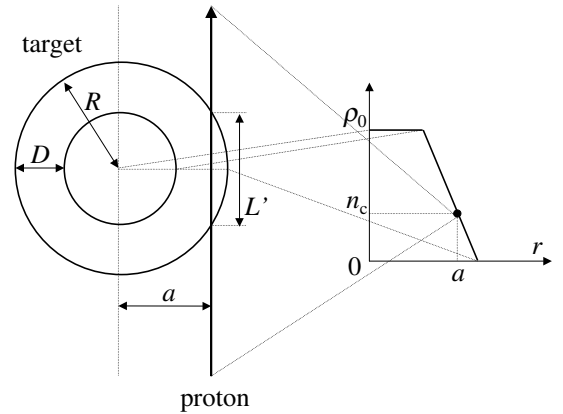


FIG. 1: Model for the density distribution of a target nucleus and the critical proton trajectory inside which the reaction with the target nucleus occurs.

top, $R - D$, as shown in Fig. 1, in such a way that they follow a typical behavior of the distributions deduced from elastic scattering data off stable nuclei [6, 18], i.e., $n_n(r = 0) + n_p(r = 0) = \rho_0 \equiv 0.16 \text{ fm}^{-3}$ and $D = 2.2$ fm. This D corresponds to the thickness parameter of about 0.53 fm in the two-parameter Fermi distribution. We then replace the optical depth by an effective one,

$$\tau = \bar{\sigma}_{pN} n_c L', \quad (3)$$

where $\bar{\sigma}_{pN} = (Z/A)\sigma_{pp} + (1 - Z/A)\sigma_{pn}$, n_c is the total nucleon density at $r = a$, and $L' = 2\sqrt{R^2 - a^2}$ is the length of the part of the critical trajectory in which the total nucleon density is larger than n_c . The value of τ is set to be 0.9 since this is consistent with the values of a_0 and n_c for ^{12}C , ^{58}Ni , ^{124}Sn , and ^{208}Pb that were deduced from the elastic scattering data (see Ref. [11] and references therein).

Let us now consider the deviation ΔX of $X = \bar{\sigma}_{pN}$, a , n_c , and L' from the value X_0 at $T_p = 800$ MeV. As long as $T_p > 100$ MeV, $\Delta \bar{\sigma}_{pN}$ is sufficiently small that

$$\tau \frac{\Delta \bar{\sigma}_{pN}}{\bar{\sigma}_{pN 0}^2} \approx -n_{c0} \Delta L' - L'_0 \Delta n_c. \quad (4)$$

Because of the assumed trapezoidal distribution, one can obtain

$$\Delta n_c = -\frac{\rho_0}{D} \Delta a. \quad (5)$$

Combining Eqs. (4) and (5), one can express the relation between $\Delta \bar{\sigma}_{pN}$ and Δa as

$$\tau \frac{\Delta \bar{\sigma}_{pN}}{\bar{\sigma}_{pN 0}^2} \approx \left(\frac{\rho_0}{D} L'_0 - \frac{dL'}{da} \Big|_0 n_{c0} \right) \Delta a. \quad (6)$$

We thus obtain

$$\sigma_R \approx \pi a_0^2 \left[1 + \left(\frac{\rho_0 a_0}{D n_{c0}} - \frac{a_0}{L'_0} \frac{dL'}{da} \Big|_0 \right)^{-1} \frac{\Delta \bar{\sigma}_{pN}}{\bar{\sigma}_{pN0}} \right]^2. \quad (7)$$

We now proceed to express the length R . In doing so, we first note the normalization condition for the assumed trapezoidal distribution,

$$A = \frac{4\pi\rho_0}{3} \left(R^3 - \frac{3}{2} DR^2 + D^2 R - \frac{1}{4} D^3 \right). \quad (8)$$

One can seek an approximate solution to this equation by setting $R = R_0 + D/2 + \delta R$, with $R_0 = (3A/4\pi\rho_0)^{1/3}$, and assuming that δR is small. One thus obtains

$$R \approx R_0 + \frac{D}{2} - R_0 \left(1 + \frac{12R_0^2}{D^2} \right)^{-1}. \quad (9)$$

From this expression, δR can be shown to be small even for light elements. Hereafter we substitute expression (9) into the reaction cross section formula (7) through L' . Note that since both a_0 and R_0 behave as $\propto A^{1/3}$, the derivative dL'/da may well be performed by assuming $R_0 \propto a$.

In Fig. 2 we compare the formula (7) with the empirical data for the reaction cross section for targets such as C, Ca, Zr, and Pb. The formula (7) in which a_0 is set to be a value determined from the measured angle of the first diffraction maximum in proton elastic scattering [11, 12] well reproduces the T_p dependence of the measured reaction cross section [14, 19] for T_p down to about 100 MeV. Remarkably, it agrees almost completely with the 100–180 MeV data updated by Auce *et al.* [19]. The T_p dependence of such data is stronger for smaller A , a feature described by the prefactor of $\Delta \bar{\sigma}_{pN}/\bar{\sigma}_{pN0}$ in Eq. (7). Below 100 MeV, the measured cross section shows resonance features and sharp decrease due to the Coulomb repulsion between the incident proton and target nucleus, both of which are not allowed for in constructing the present formula. The neglect of the Coulomb corrections is reasonable above 100 MeV, since the empirical reaction cross section for protons on stable nuclei is appreciably lower than that for neutrons only at incident energy lower than ~ 70 MeV [20]. Below 100 MeV, there is another limitation that faces the formula (7): σ_{pn} is too large to make the formula applicable [16]. We remark that the data above 200 MeV, tabulated in Ref. [14], have to be seen with caution. This is partly because the recent data at energies between 80 and 180 MeV [19] are not smoothly connected with the data above 200 MeV and partly because the data between 200 MeV and 600 MeV are systematically larger than the data at 860 MeV, in contrast to the tendency of the nucleon-nucleon total cross section [15, 16]. We also remark that the previous predictions based on microscopic optical potential models [17, 21, 22] are more sensitive to T_p than ours in a way more difficult to reproduce the T_p dependence of the data. In fact, such models involve the exponential σ_{pN}

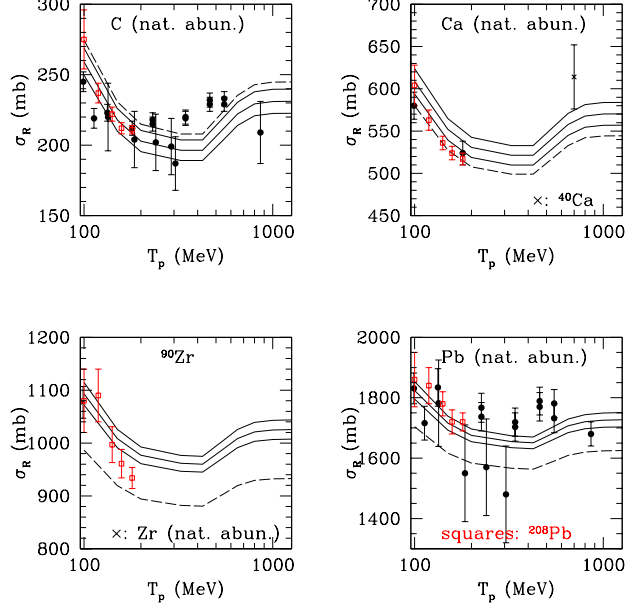


FIG. 2: (Color online) The proton-nucleus reaction cross section as a function of proton incident energy. The target nucleus is natural C, natural Ca, ^{90}Zr , and natural Pb. The squares denote the data from Auce *et al.* [19], while the filled circles and crosses denote the data tabulated in Ref. [14]. Note some exceptions in which the target nucleus is slightly different in mass number: crosses for ^{40}Ca and natural Zr and squares for ^{208}Pb . The lines are the results from the formula (7) in which a_0 is set to be $1.214A^{1/3}$ fm (dashed lines), 2.7 fm (bold line for C), 2.65 fm (lower, thin line for C), 2.75 fm (upper, thin line for C), 4.25 fm (bold line for Ca), 4.2 fm (lower, thin line for Ca), 4.3 fm (upper, thin line for Ca), 5.7 fm (bold line for Zr), 5.65 fm (lower, thin line for Zr), 5.75 fm (upper, thin line for Zr), 7.4 fm (bold line for Pb), 7.35 fm (lower, thin line for Pb), and 7.45 fm (upper, thin line for Pb). The choice of 2.65–2.75 fm for C, 4.2–4.3 fm for Ca, 5.65–5.75 fm for Zr, and 7.35–7.45 fm for Pb is based on the measured diffraction peak angle in proton elastic scattering.

dependence in the prediction of the reaction cross section through the phase shift function, in contrast to the power-law σ_{pN} dependence of the formula (7).

From Fig. 2 we can also examine to what extent a simple choice of a_0 as $1.214A^{1/3}$ fm works in the cross section formula. As was seen from Ref. [12], this simple scaling well reproduces the values of a_0 determined from the measured angle of the first diffraction maximum in proton elastic scattering for stable nuclei ranging from light to heavy elements. In fact, we see a good agreement between the results for the cross section formula from both choices of a_0 , although the values from the simple $A^{1/3}$ scaling tend to be lower than those from the other by typically 5–10 % for $A \gtrsim 100$.

As far as the A dependence is concerned, the present formula is similar to the parametrization constructed by Kox *et al.* [23]. However, they differ significantly in the

way of describing the energy dependence. Kox *et al.* introduced a semiempirical energy dependent parameter that takes care of changing “surface transparency” as the projectile energy changes, while the energy dependence of our formula stems solely from that of $\bar{\sigma}_{pN}$ and hence our formula is free from any adjustable energy dependent parameter. We remark that the formula by Kox *et al.* is applicable for a wider range of the incident energy including the low energy region where the Coulomb repulsion between the projectile and target takes effect, although it ignores resonance features which are also important in such a low energy region.

We now extend the cross section formula (7) constructed for stable nuclei to unstable nuclei by introducing the dependence on the neutron excess δ . In doing so, we first note a formula for the rms radii of proton and neutron point distributions, R_p and R_n , which reads

$$R_p = c_1 A^{1/3} + c_2 + c_3(\delta - \delta_0)^2, \quad (10)$$

with $c_1 = 0.915$ fm, $c_2 = -0.102$ fm, $c_3 = 0.389$ fm, and $\delta_0 = 0.880$, and

$$R_n = c_4 A^{1/3} (1 + c_5 L \delta^2 + c_6 L^2 \delta^4) + c_7 + c_8 \delta, \quad (11)$$

with $c_4 = 0.880$ fm, $c_5 = 0.00635$ MeV $^{-1}$, $c_6 = -0.000172$ MeV $^{-2}$, $c_7 = 0.302$ fm, and $c_8 = 0.193$ fm. This formula was constructed in Ref. [2] by fitting the calculations obtained from macroscopic nuclear models for $A > 50$, $0 < \delta < 0.3$, and various values of the density symmetry coefficient L and the incompressibility K_0 of symmetric nuclear matter. It was noted that the calculated results for the rms radii are almost independent of K_0 . We remark that the formulas (10) and (11), when extrapolated into the range of $4 \leq A \leq 50$, reproduces as well the values of the rms charge and matter radii deduced from elastic scattering data for stable nuclei.

The formulas (10) and (11) imply the significance of allowing for uncertainties in the density symmetry coefficient L in describing the size dependent quantities at finite neutron excess. In fact, L acts to increase the nuclear size at nonzero δ . This is mainly because the saturation density of uniform nuclear matter at finite neutron excess decreases from that in the symmetric case in such a way that the decrease is roughly proportional to $L\delta^2$ [2]. This effect of L could be seen by systematically analyzing the first diffraction maxima in the proton elastic scattering data [24] and thus could manifest itself more remarkably in the reaction cross section which behaves as the size squared.

In order to describe the cross section at finite neutron excess by including the effect of L , we multiply expression (7) by a scale factor $f(A, \delta; L) = R_m^2(A, \delta; L) / R_m^2(A, \delta = 0; L)$ with the rms matter radius $R_m = \sqrt{(N/A)R_n^2 + (Z/A)R_p^2}$. This is reasonable, because, at least for stable nuclei heavier than $A \sim 50$, the rms matter radii deduced in previous elaborate analyses from elastic scattering data agree very well with $\sqrt{3/5}a$

[11]. Although this agreement neither holds for $A \lesssim 50$ [12] nor is obvious at large neutron excess, it is natural to expect that the isospin dependence of R_m is similar to that of a . We remark in passing that the scale factor f is sufficiently close to unity for stable nuclei including ^{208}Pb that it does almost no damage to the good agreement between the formula and the data.

In addition to the isospin dependence coming through this scale factor, another isospin dependence is inherent in the formula (7) through the part associated with $\bar{\sigma}_{pN}$. In the absence of detailed information about the surface diffuseness and neutron skin at large neutron excess, we simply leave it as it is. This is expected to be good enough since σ_{pp} and σ_{pn} are not so different at $T_p = 100$ –1000 MeV as to affect the analysis of the reaction cross section data within the error bars, which are typically of order a few percent.

In the black sphere picture adopted here, possible neutron halos have no influence on the construction of the cross section formula for unstable nuclei. This is because such halos correspond to a very low density region which is “optically” very thin. Moreover, the macroscopic nuclear models leading to Eqs. (10) and (11) do not allow for the possible presence of a neutron halo [2]. If the cross section formula is significantly smaller than the empirical value for halo nuclei for reasonable values of L , therefore, this would signify the limitation of the present framework and the enhancement of the reaction cross section due to the presence of halos.

We now focus on the interaction cross section data for a halo nucleus ^{11}Li [25] as well as the reaction cross section data for helium isotopes [9]. Note that the interaction cross section can be regarded as equal to the reaction cross section for halo nuclei in which internucleon excitations generally involve breakup of halo neutrons. Such light elements are expected to be suitable for examining the isospin dependence, partly because for stable nuclei a_0 is consistent with $1.214A^{1/3}$ fm, and partly because f can amount to about 1.1. In fact, the formula (7) with $a_0 = 1.214A^{1/3}$ fm well reproduces the data for ^4He [26] and Li of the natural abundance [27]. From the formula (7) further multiplied by the scale factor f with a typical L value of 100 MeV, we obtain a smaller value for ^{11}Li by about 10 %, but a value consistent with the empirical data for halo nuclei ^6He and ^8He . It might be tempting to attribute this deviation for ^{11}Li to the presence of a neutron halo, since the formula (7) and the scale factor f are not influenced by an extremely low density tail of the neutron distribution. However, this attribution is not obvious because of the consistency obtained for ^6He and ^8He which are known to have a similar three-body structure to that of ^{11}Li [28].

So far we have assumed that nuclei are spherical. Nuclear deformation, however, does affect the reaction cross section and thus might be deduced from the experimental data measured for heavy deformed nuclei. For simplicity, we focus on quadrupolar deformation and describe a nucleus as a static ellipsoid having the length, b_1 , b_1 , b_2 ,

of the three axes. Both for prolate ($b_1 < b_2$) and oblate ($b_1 > b_2$) deformations with random orientations, the cross section seen by incident protons becomes, on the average, larger than the value for a sphere of the same volume. The relative increment can be calculated as

$$g = \frac{2}{5} \alpha_2^2 + \dots, \quad (12)$$

where α_2 is the quadrupolar deformation factor satisfying $b_2/b_1 = (1 + \alpha_2)/(1 - \alpha_2/2)$. This suggests that even for large deformation $|\alpha_2| \sim 0.2$, g amounts to about 2 % only.

In the above estimate of the effect of deformation, we ignore possible rotation of the nucleus. Since the rotation speed is far smaller than the speed of light, it is reasonable to consider that the incident protons, which move relativistically, see the target nucleus nonrotating during the flight. However, rotation would tend to enlarge the nucleus itself. Balance between the centrifugal force and the nuclear incompressibility would typically give rise to about a percent enhancement of the cross section. We can thus conclude that the combined effect of deformation and rotation is significantly smaller than the effect of large neutron excess.

III. FORMULA FOR NUCLEUS-NUCLEUS REACTION CROSS SECTION

In this section we generalize the formula constructed in Sec. II to the case of nucleus-nucleus reaction cross section. As in Ref. [12], we straightforwardly set it as

$$\sigma_R = \pi(a_P + a_T)^2, \quad (13)$$

where a_P and a_T are the black sphere radii of the projectile (Z_P, A_P) and target (Z_T, A_T) nucleus. By following a line of argument for the proton-nucleus case, we obtain

$$\sigma_R = \pi \left[(a_{P0} + \Delta a_P) f_P^{1/2} + (a_{T0} + \Delta a_T) f_T^{1/2} \right]^2, \quad (14)$$

where f_P and f_T are the scale factors for the projectile and target nucleus, and Δa_P and Δa_T are the deviations of a_P and a_T from the values of a_{P0} and a_{T0} at incident energy per nucleon of 800 MeV, both of which are determined from Eq. (6) in which $\bar{\sigma}_{pN}$ is replaced by

$$\begin{aligned} \bar{\sigma}_{NN} = & \left(\frac{Z_T}{A_T} \right) \left[\left(\frac{Z_P}{A_P} \right) \sigma_{pp} + \left(1 - \frac{Z_P}{A_P} \right) \sigma_{pn} \right] \\ & + \left(1 - \frac{Z_T}{A_T} \right) \left[\left(\frac{Z_P}{A_P} \right) \sigma_{pn} \right. \\ & \left. + \left(1 - \frac{Z_P}{A_P} \right) \sigma_{pp} \right] \end{aligned} \quad (15)$$

for Δa_T and ($T \leftrightarrow P$) for Δa_P . Here we have omitted the effects of nuclear deformation. The formula (14) reduces to the proton-nucleus case by setting either a_P or a_T to

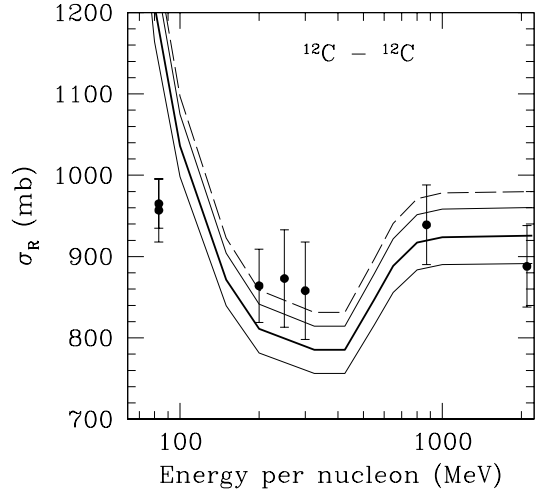


FIG. 3: The ^{12}C - ^{12}C reaction cross section as a function of energy per nucleon. The filled circles are the empirical data from Refs. [23, 26, 29]. The lines are the results from the formula (14) in which a_0 is set to be 2.7 fm (bold), 2.65 fm (lower, thin), 2.75 fm (upper, thin), and $1.214A^{1/3}$ fm (dashed). The choice of 2.65–2.75 fm is based on the measured diffraction peak angle in proton elastic scattering.

be zero. Hereafter we will set $a_{P0} = 1.214A_P^{1/3}$ fm and $a_{T0} = 1.214A_T^{1/3}$ fm unless notified otherwise.

The formula (14) works well for the ^{12}C - ^{12}C case for energy per nucleon at least down to 200 MeV (see Fig. 3). In fact, in this energy range the empirical values of the ^{12}C - ^{12}C case [23] are almost four times as large as those of the p - ^{12}C case, while the formula (14) for the ^{12}C - ^{12}C case is just four times as large as that for the p - ^{12}C case. At lower energies, the formula (14) overestimates the reaction cross section to an extent much larger than the one that could be explained by our neglect of the Coulomb repulsion. This suggests the necessity of modifying the classical optical depth argument underlying the formula (14) in analyzing the low energy nucleus-nucleus reactions. The agreement for energy per nucleon down to 200 MeV and the deviation for lower energy can also be seen in all the other reactions between stable nuclei tabulated in Table II of Ref. [23].

We note that for the ^{4}He - ^{12}C case, the formula (14) significantly overestimates the reaction cross section even at energy per nucleon of order or higher than 800 MeV as can be seen by comparison with the empirical data [26]. This exceptional behavior is attributable to the fact that excitations associated with internucleon motion are highly suppressed in α particles.

It is important to compare the constructed formula with the empirical data for unstable nuclei incident on a stable nucleus target. We note the data for the interac-

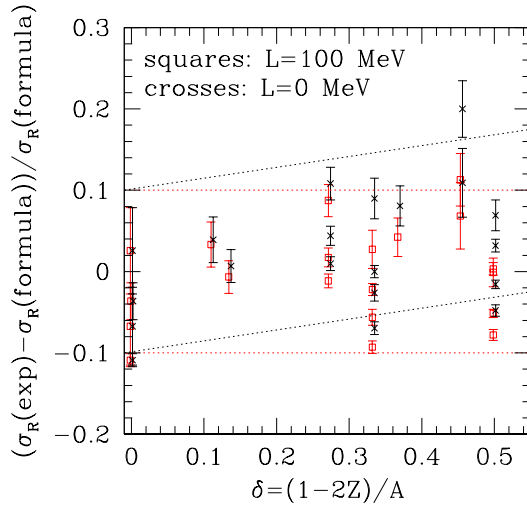


FIG. 4: (Color online) Deviation of the empirical reaction cross section from the cross section formula (14) with $L = 0$ MeV (crosses) and $L = 100$ MeV (squares). a_{P0} and a_{T0} are set to be $1.214A_P^{1/3}$ fm and $1.214A_T^{1/3}$ fm, respectively. The dotted lines are drawn to guide the eye.

tion cross section at energy per nucleon of order 800 MeV tabulated in Ref. [10]. For candidates of halo nuclei such as ^6He , ^8He , ^{11}Li , ^{11}Be , and ^{19}C , we may assume that the interaction cross section is almost equal to the total reaction cross section. For a typical value of L of order 100 MeV, we obtain a good agreement between the formula and the data for Be, C, and Al targets; the difference is of order 5 %, typically. The results from these comparisons, together with the aforementioned proton-nucleus cases (^{11}Li [25], ^4He [9, 26], ^6He [9], natural Li [27], ^9Be [27], natural C [27]), are summarized in Fig. 4. We find that the deviation between the empirical data and the formula with $L = 100$ MeV is within ± 10 %, while the formula with $L = 0$ MeV tends to underestimate the cross section at large neutron excess. Judging from the scattering pattern in the plot for $L = 100$ MeV,

which is almost uniform within the band between ± 10 %, and recalling that the formula is not influenced by the presence of neutron halos, we see no absolute need for taking into account the possible enhancement of the reaction cross section by an extremely low density tail of the neutron distribution in explaining the empirical values of the reaction cross section. In the absence of this enhancement, it is expected that one can deduce the value of L from the comparison between the empirical data and the formula. We note, however, that the difference of the formula with $L = 100$ MeV from the formula with $L = 0$ MeV is of order or even smaller than that from the empirical data. This suggests the necessity of a systematic analysis in deducing the value of L itself.

IV. CONCLUSION

We constructed a formula for the proton-nucleus reaction cross section in a way free from any adjustable T_p dependent parameter. The dependence of the cross section on A and T_p was deduced by combining the black sphere picture of nuclei with a simple argument of the proton optical depth. For stable nuclei, this formula remarkably well reproduces the empirical T_p dependence of the reaction cross section at $T_p = 100\text{--}1000$ MeV. This suggests a great advantage over previous microscopic optical potential models in which the T_p dependence becomes too strong through the phase shift function to reproduce the empirical behavior. In addition, we took into account the effects of large neutron excess typical of unstable nuclei and nuclear deformation on the reaction cross section. We thus found out a possible way of examining the influence of the density dependence of the symmetry energy and the presence of neutron halos on the reaction cross section.

Acknowledgments

We acknowledge the members of Japan Charged-Particle Nuclear Reaction Data Group (JCPRG), especially N. Oyamatsu, for kindly helping us collect various data sets.

[1] A.W. Steiner, M. Prakash, J.M. Lattimer, and P.J. Ellis, Phys. Rep. **411**, 325 (2005).
[2] K. Oyamatsu and K. Iida, Prog. Theor. Phys. **109**, 631 (2003).
[3] G.D. Alkhazov, S.L. Belostotsky, and A.A. Vorobyov, Phys. Rep. **42**, 89 (1978).
[4] A. Chaumeaux, V. Layly, and R. Schaeffer, Ann. Phys. (N.Y.) **116**, 247 (1978).
[5] G.J. Igo, Rev. Mod. Phys. **50**, 523 (1978).
[6] C.J. Batty, E. Friedman, H.J. Gils, and H. Rebel, Adv. Nucl. Phys. **19**, 1 (1989).
[7] B. Frois, C.N. Papanicolas, and S.E. Williamson, in *Modern Topics in Electron Scattering*, edited by B. Frois and I. Sick (World Scientific, Singapore, 1991), p. 352.
[8] A.A. Korsheninnikov *et al.*, Nucl. Phys. **A617**, 45 (1997).
[9] S.R. Neumaier *et al.*, Nucl. Phys. **A712**, 247 (2002).
[10] A. Ozawa, T. Suzuki, and I. Tanihata, Nucl. Phys. **A693**, 32 (2001).
[11] A. Kohama, K. Iida, and K. Oyamatsu, Phys. Rev. C **69**, 064316 (2004).
[12] A. Kohama, K. Iida, and K. Oyamatsu, Phys. Rev. C **72**, 024602 (2005).

- [13] A. Kohama, K. Iida, and K. Oyamatsu (unpublished).
- [14] W. Bauhoff, At. Data Nucl. Data Tables **35**, 429 (1986).
- [15] R.A. Arndt, L.D. Roper, R.A. Bryan, R.B. Clark, B.J. VerWest, and P. Signell, Phys. Rev. D **28**, 97 (1983).
- [16] W.N. Hess, Rev. Mod. Phys. **30**, 368 (1958).
- [17] L. Ray, Phys. Rev. C **20**, 1857 (1979).
- [18] H. de Vries, W. de Jager, and C. de Vries, At. Data Nucl. Data Tables **36**, 495 (1987).
- [19] A. Auce *et al.*, Phys. Rev. C **71**, 064606 (2005).
- [20] M.B. Chadwick *et al.*, Nucl. Sci. Eng. **131**, 293 (1999).
- [21] D.J. Ernst, Phys. Rev. C **19**, 896 (1979).
- [22] P.K. Deb, B.C. Clark, S. Hama, K. Amos, S. Karataglidis, and E.D. Cooper, Phys. Rev. C **72**, 014608 (2005).
- [23] S. Kox *et al.*, Phys. Rev. C **35**, 1678 (1987).
- [24] K. Iida, K. Oyamatsu, and B. Abu-Ibrahim, Phys. Lett. **B576**, 273 (2003).
- [25] I. Tanihata *et al.*, Phys. Lett. **B287**, 307 (1992).
- [26] J. Jaros *et al.*, Phys. Rev. C **18**, 2273 (1978).
- [27] A. Johansson, U. Svandberg, and O. Sundberg, Arkiv Fysik **19**, 527 (1961).
- [28] L.V. Chulkov *et al.*, Nucl. Phys. **A759**, 43 (2005).
- [29] T. Zheng *et al.*, Nucl. Phys. **A709**, 103 (2002).